Synthesis, electrochemistry and spectroelectrochemistry of a porphyrin–viologen donor–acceptor diad†

Matthew T. Barton,[a] Natalie M. Rowley,*[a] Peter R. Ashton,[a] Christopher J. Jones,[a] Neil Spencer,[a] Malcolm S. Tolley[a] and Lesley J. Yellowlees[b]

[a] *School of Chemistry, University of Birmingham, Edgbaston, Birmingham, UK B15 2TT*
E-mail: N.M.Rowley@bham.ac.uk
[b] *Department of Chemistry, University of Edinburgh, Edinburgh, UK EH9 3JJ*

Received (in Cambridge, UK) 31st March 2000, Accepted 12th May 2000
Published on the Web 15th June 2000

A new donor–acceptor (D–A) molecule, 5,10,15,20-[*N*-benzyl-*N*′-(4-benzyl-4,4′-bipyridinium-4-pyridyl)]-triphenylporphyrin tris(hexafluorophosphate), **4**, has been synthesised. The diad, **4**, and its precursors, have been fully characterised by ^{1}H and ^{13}C NMR spectroscopy, mass spectrometry, UV/Visible spectroscopy and cyclic voltammetry. *In-situ* UV/Visible and EPR measurements show that the site of the first electrochemical reduction is the benzylviologen component of the molecule. The second reduction wave from cyclic voltammetry was shown by *in-situ* EPR to comprise two unresolved one-electron processes, and this was confirmed by chronocoulometry. The first of these two reduction processes rendered the diad diamagnetic, as was shown by the disappearance of the signal due to the benzylviologen radical. The second gave rise to the appearance of a new EPR signal, which was found to correspond to the porphyrin radical. We believe this to be the first reported resolved spectrum of a monoreduced porphyrin radical.

We have previously synthesised a series of peripherally-metallated porphyrins and reported their photochemical properties.[1–3] It was found that these complexes undergo rapid electron transfer from the excited singlet state of the porphyrin to the [Mo(Tp^{Me,Me})(NO)Cl] acceptor moiety [where Tp^{Me,Me} is hydrotris(3,5-dimethylpyrazolyl)borate]. These are very rare examples of electron transfer to external, but covalently-linked, transition metal based redox centres.

Wrighton *et al.*[4] have previously demonstrated intramolecular electron transfer in a covalently linked porphyrin–viologen diad by resonance Raman spectroscopy. They reported an electron transfer rate of *ca.* 8×10^{7} s^{-1}— this relatively small value being consistent with the low driving force (ΔG^{0} *ca.* −0.4 eV) and the large distance between donor and acceptor. More recently, Yonemoto *et al.*[5] have shown that donor–acceptor complexes of the type [(2,2′-bipy)$_2$Ru{4-CH$_3$-2,2′-bipy-4′)(CH$_2$)$_n$(4,4′-H$_2$bipy-CH$_3$)]$^{4+}$ (n = 2–5, 7, 8) can be exchanged onto the surface of large-pore zeolites (Y, L and mordenite). From solid state CP-MAS spectra of ^{13}C-labelled compounds, it was established that these diads occupy surface sites, in which the acceptor end is occluded by the zeolite channels, while the size-excluded donor end is exposed. It was also found that the back electron transfer reaction is approximately 10^{5} times slower for diads on the zeolite surface than in solution.

As outlined above, we have already successfully synthesised donor–acceptor systems which undergo photoinduced electron transfer, generating charge-separated states with lifetimes of the order of several hundred picoseconds. We now wish to develop novel systems which give rise to longer lifetimes of the photoinduced charge-separated states. In order to achieve this, we have constructed diad systems capable of occlusion by zeolite Y, in the hope that our systems will behave in a similar manner to those of Yonemoto *et al.*[5] In this paper we report the synthesis, characterisation, electrochemistry and spectroelectrochemistry of a new porphyrin-based donor–acceptor compound and its precursors. The target molecule comprises a porphyrin, covalently attached to a dibenzylviologen acceptor unit, the acceptor end of which is sufficiently small to be occluded by large pore zeolites, such as zeolite Y.

† Electronic supplementary information (ESI) available: UV/Visible spectra of **1**–**4** and cyclic voltammogram of **4**. See http://www.rsc.org/suppdata/nj/b0/b002589p/

Results and discussion

Synthesis and characterisation of compounds 1–4

Synthesis. Compounds **1** to **4** are illustrated in Fig. 1. Porphyrin **1** was prepared by an Adler-type condensation of pyrrole, benzaldehyde and pyridine-4-carbaldehyde.[6] The molar ratio of reactants (1 : 1.18 benzaldehyde to pyridine-4-carbaldehyde) was found to give the highest yield, after purification by column chromatography, of the mono-substituted porphyrin. Compound **2** was prepared by mono-substitution of 4,4′-bipyridyl. The reaction was performed in toluene, by slow addition of benzyl bromide to an excess of 4,4′-bipyridyl. Counter-ion exchange then gave the desired organic-soluble product. Compound **3** was prepared by quaternisation of the pyridyl moiety of compound **1**. A large excess of α,α′-dibromo-*p*-xylene was added to increase the yield of the monosubsitited α,α′-dibromo-*p*-xylene product. Quaternisation of **2** on reaction with **3** gave compound **4**, again using a large excess of **2**. Counter-ion exchange then gave the desired organic-soluble product. ^{1}H NMR spectroscopy, LSIMS and elemental analyses confirm the identity of all of the reported compounds.

^{1}H NMR Spectra. In general, the solution ^{1}H NMR spectra of compounds **1**–**4** were well-resolved and easily assigned. Large shifts were seen due to the presence of quaternised nitrogen atoms and the ring-current effect of the porphyrin macrocycle. These generally shifted signals to very high frequency, except for internal porphyrin N*H* protons which were shifted to low frequency by the ring current.

^{13}C NMR Spectra. The spectrum of **4** has been partially

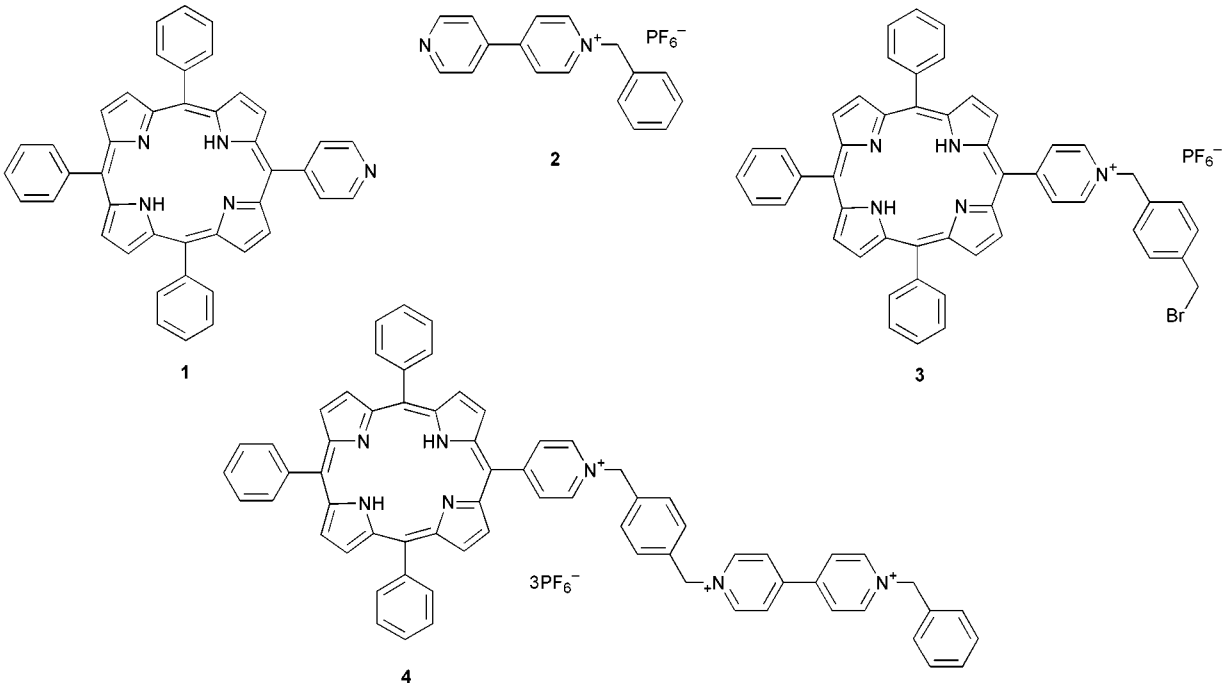

Fig. 1 Structures of compounds **1** to **4**.

assigned by means of 2-dimensional NMR (HSQC) and PENDANT experiments. The assignment of quaternary carbon environments is incomplete (peaks listed in curly brackets in Experimental section).

Electronic absorption spectra. The electronic spectral data for compounds **1**–**4** are shown in Table 1. In dichloromethane, the porphyrin-based compounds show absorption spectra characteristic of the porphyrin group, with five major absorptions: the intense B or Soret band at around 420 nm, and four Q bands in the range 500–650 nm which decrease in intensity with increasing wavelength. Compound **3** shows an additional absorption at 235 nm, corresponding to addition of the xylene moiety. The absorption due to the acceptor component (266 nm in **2**) combines with this xylene absorption to give a broader band at 257 nm when present in **4**.

In general, the spectrum of **4** is a simple addition of the spectra of its components, indicating that there is little or no ground state electronic interaction between the components of the diad, when assembled. This is encouraging with respect to using these compounds as photoactive devices, since it implies that electron transfer should not take place until the molecule is photochemically promoted to its excited state.

Cyclic voltammetry. The electrochemistry of compounds **1**–**4** was investigated by cyclic voltammetry in a 0.2 mol dm^{-3} solution of [*n*-Bu_4N][BF_4] in dry dichloromethane (Table 2). The electrochemistry of **4** was also studied in an acetonitrile solution.

Compound **1** shows two reversible reductions and one irreversible oxidation, at the expected values for a porphyrin. Presumably the second oxidation expected for a free-base porphyrin is masked by solvent breakdown (*i.e.* beyond around +1.50 V). Compound **2** exhibits two reversible reductions at the potentials expected for a viologen-type moiety. Compound **3** exhibits a single reversible reduction at −0.70 V, which is attributed to the first reduction of the pyridinium porphyrin moiety, being similar in potential to the second reduction potential observed in **4** (*vide infra*). No second reduction potential of the pyridinium porphyrin entity was observed, possibly as a result of being masked by solvent breakdown. The two oxidation processes expected for a porphyrin entity could not be observed.

On assembly of **2** and **3** to make compound **4**, the waves of the different components add to give the observed five redox processes. Two oxidation processes are observed. The first oxidation is assigned to the porphyrin entity. It is at a less positive potential compared to **1** and is irreversible. The second oxidation is presumably due to the decomposition product of the first oxidation process. The first reduction (−0.18 V) is reversible and is assigned to the acceptor moiety. Chronocoulometry at −0.30 V confirms that this first reduction process involves one electron. The reversible process at −0.70 V has a large current and coulometric experiments confirm that this process involves two electrons. Further experiments (*vide infra*) confirm that the reduction process at −0.70 V consists of two one-electron processes which occur at very similar potentials and cannot be resolved under these

Table 1 Electronic spectral data in dichloromethane for compounds **1** to **4**

	B $\lambda^a(\varepsilon)^b$	$Q_y(1,0)$ $\lambda^a(\varepsilon)^c$	$Q_y(0,0)$ $\lambda^a(\varepsilon)^c$	$Q_x(1.0)$ $\lambda^a(\varepsilon)^d$	$Q_x(0,0)$	
					$\lambda^a(\varepsilon)^d$	$\lambda^a(\varepsilon)^c$
1	415(2.4)	513(1.7)	547(6.5)[d]	587(4.6)	644(2.7)	
2						266(5.2)
3	414(1.4)	516(1.2)	570(1.0)	585(8.7)	653(4.9)	235(1.6)[b]
4	416(8.3)[c]	518(1.2)	565(1.1)	588(8.6)	651(5.8)	257(3.9)

[a] In nm. [b] ε in $mol^{-1}\,l\,cm^{-1} \times 10^5$. [c] ε in $mol^{-1}\,l\,cm^{-1} \times 10^4$. [d] ε in $mol^{-1}\,l\,cm^{-1} \times 10^3$.

Table 2 Electrochemical data of compounds **1**–**4**[a]

		Oxidation		Reduction		
	Solvent	$E_f(\Delta E_p)$	$E_f(\Delta E_p)$	$E_f(\Delta E_p)$	$E_f(\Delta E_p)$	$E_f(\Delta E_p)$
1	CH_2Cl_2	+1.16[b]		−1.05(100)	−1.40(100)	
2	CH_2Cl_2			−0.76(109)	−1.47(160)	
3	CH_2Cl_2			−0.70(56)		
4	CH_2Cl_2	+0.95[b]	+1.35[b]	−0.18(63)	−0.70(150)	−1.63[b]
4	MeCN	+0.66[b]	+0.97[b]	−0.30(102)	−0.78(78)	−1.70[b]

[a] All measurements were made by cyclic voltammetry, in the solvent specified, containing 0.2 mol dm^{-3} [*n*-Bu_4N][BF_4] at a platinum bead working electrode. The scan rate was 200 mV s^{-1}. All potentials are *vs.* SCE. The ferrocenium–ferrocene couple was used as an internal reference (0.55 ± 0.01 V). Values in parentheses are peak–peak separation in mV for the reversible processes. (ΔE_p for the ferrocenium–ferrocene couple under the same conditions was about 120 mV). [b] Denotes an irreversible process.

conditions. The irreversible reduction at −1.63 V is porphyrin-based and leads to the formation of two product waves on the return sweep (at −0.96 V and −1.16 V).

Cyclic voltammetry measurements were also recorded for **4** in acetonitrile. A shift, when compared to dichloromethane solutions, of *ca.* 100 mV to more negative potential was seen for the reduction processes, and of *ca.* 300 mV to less positive potential for the oxidation processes. This is probably due to the change in solvent, since the ferrocene couple was also shifted.

Spectroelectrochemistry. *In-situ* electronic absorption spectra of **4** were recorded from a 0.1 mol dm^{-3} solution of [*n*-Bu_4N][BF_4] in dry acetonitrile at 253 K. From cyclic voltammetry, two reversible reduction processes are seen in acetonitrile, at −0.30 V and −0.78 V, and were investigated. The irreversible process at −1.70 V was not investigated.

During the first reduction Fig. 2, when the potential is set to −0.61 V, no significant change is seen in the Soret band or the four Q bands. However, the band at 260 nm decreases dramatically in intensity and a new, broad absorption is seen at around 890 nm together with a shoulder at 300 nm. This first reduction process is therefore assigned to the acceptor component of the molecule as the characteristic absorption bands of the porphyrin moiety remain relatively unaltered following bulk reduction at −0.61 V. The reduction process is reversible under these conditions since the original spectrum is recovered by returning the potential to +0.20 V.

Upon controlled potential reduction at −1.40 V the Soret band collapses and broadens and the Q bands also collapse. New absorptions develop at around 380 nm and 450 nm. These spectral changes indicate that a porphyrin-based reduction takes place at this potential and under these conditions the process is irreversible, since the original spectrum cannot be regenerated in this solvent and at this temperature by setting the potential back to +0.20 V. Later evidence (*vide infra*) shows that two electrons are transferred during the process at −0.78 V.

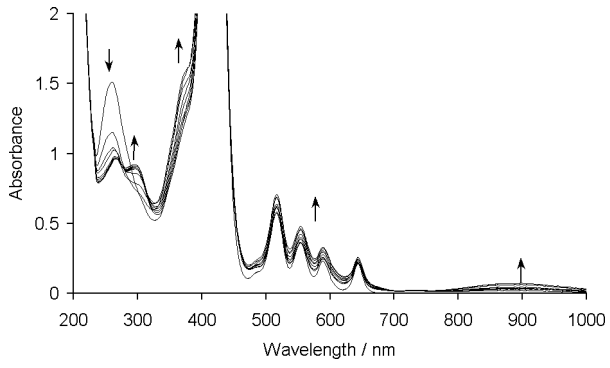

Fig. 2 Electronic spectra recorded during reduction of **4** to $\mathbf{4}^-$.

EPR Spectral studies. The site of the first reduction process of **4** was confirmed as the viologen by using *in-situ* EPR spectroscopy in a 1.0 M solution of [*n*-Bu_4N][BF_4] in DMF at 233 K. When the controlled potential is set to −0.61 V a signal develops at $g = 2.012$ which is indicative of formation of a radical anion species (Fig. 3). The signal shows around 27 resolved lines. Simulations (Fig. 3) demonstrate that this is attributed to coupling with three N atoms (we infer then that these are the acceptor N atoms, $a^N = 4.08$ G), six H atoms ($a^H = 1.41$ G) and a further six H atoms ($a^H = 1.00$ G). Consideration of the structure of **4** would suggest that the redox site at −0.30 V should be attributed to the acceptor part of the compound which has three equivalent nitrogen sites (the porphyrin ring having four equivalent nitrogen sites). It is likely that six H couplings observed in the EPR spectrum are due to the methylene protons (2 per nitrogen) and six are aromatic protons (again 2 per nitrogen) adjacent to N, although a detailed assignment of EPR coupling to specific H atoms requires further study. This demonstrates that the dibenzylviologen moiety is the first site of reduction, and therefore the most likely receptor for the transferred electron in the photoinduced electron transfer process.

On application of a potential of −1.40 V, the EPR signal decays as the system becomes diamagnetic. Thus the second electron enters the same orbital as the first on the acceptor part of the compound giving rise to a diamagnetic species. We would suggest that the diamagnetic species generated with the

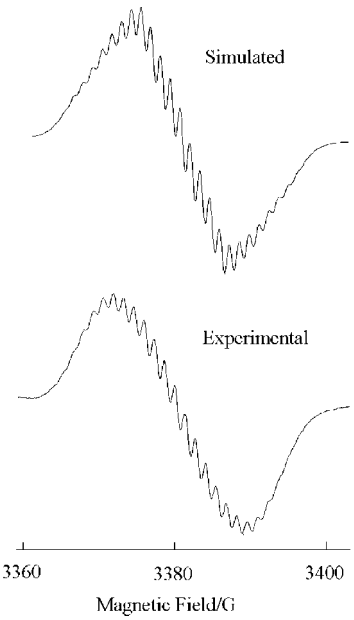

Fig. 3 *In-situ* EPR spectrum recorded during reduction of **4** to $\mathbf{4}^-$ at −0.61 V in DMF at 233 K and simulated EPR spectrum. Simulation of $\mathbf{4}^-$ used parameters in text with a Lorentzian linewidth of 1.0 G.

second reducing electron is a genuine diamagnetic species, where the second reduction electron has entered the same orbital as the first reduction electron, and is therefore not a coupled biradical. The evidence for this is the potential separation of the two reduction processes by 520 mV, which is typical of the potential difference for two electrons pairing up in the same molecular orbital. Thus the first reduction electron enters an antibonding molecular orbital based on the viologen part of the molecule, and the second reduction electron enters the same orbital, spin pairs, and therefore the molecule is diamagnetic. A new signal subsequently develops as a third electron is added to the molecule, indicating that the process seen at -0.78 V in cyclic voltammetry in acetonitrile consists of two unresolved one-electron processes (Fig. 4). The third reduction electron enters a molecular orbital on the porphyrin part of the molecule, hence the species once again becomes paramagnetic. After the third electron is added, the EPR signal has 13 lines and is centred at $g = 2.012$. In this case, simulations (Fig. 4) show that the signal shape may be modelled by coupling to four equivalent N atoms (presumably porphyrin-based, $a^{N} = 2.70$ G) and one further N atom (presumably pyridinium, $a^{N} = 5.40$ G). Reversal of the applied potential to -0.61 V shows collapse of the signal at $g = 2.012$ to give a featureless EPR spectrum and then growth of the first signal at $g = 2.012$. The EPR experiments show that at 233 K compound **4** is stable in redox states $\mathbf{4}^{-}$, $\mathbf{4}^{2-}$ and $\mathbf{4}^{3-}$. As far as we are aware this is the first reported resolved spectrum of the reduced porphyrin radical. Previous studies report only a broad unresolved signal for the monoreduced porphyrin radical.[7,8] We were surprised that this was the first example we could find in the literature of a resolved EPR spectrum of a monoreduced porphyrin radical. Previous reports show a broad signal with a peak width of around 12 G, whereas our spectrum has a peak width of 1 G, which explains why we observe coupling to the nitrogen centres, whereas earlier spectra were unresolved.

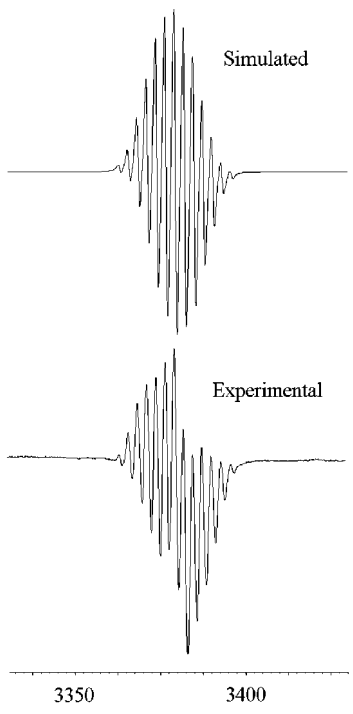

Fig. 4 *In-situ* EPR spectrum recorded during reduction of $\mathbf{4}^{2-}$ to $\mathbf{4}^{3-}$ at -1.40 V in DMF at 233 K and simulated EPR spectrum. Simulation of $\mathbf{4}^{3-}$ used parameters in text with a Lorentzian linewidth of 1.0 G.

Experimental

General details

All reagents were purchased from Aldrich and were used without further purification. Reaction solvents were deoxygenated and dried by standard methods before use. Compounds were purified by column chromatography (column lengths *ca.* 0.3 m) using Kiesel gel 60 (Merck 5554; 70–230 mesh). ^{1}H NMR spectra were recorded using a Bruker AC300 (300 MHz) or Bruker AMX400 (400 MHz) spectrometer. ^{13}C NMR spectra were recorded using a Bruker DRX500 (125 MHz) or Bruker AMX400 (100 MHz) spectrometer and assignments were made using a combination of both PENDANT and HSQC experiments.

Low resolution liquid secondary ion mass spectra (LSIMS) were obtained from a VG Zabspec mass spectrometer utilising a *m*-nitrobenzyl alcohol matrix and scanning in the positive ion mode at a speed of 5 seconds per decade. Absorption spectra were obtained using a Shimadzu UV-240 spectrophotometer. Solvent background corrections were made in all cases.

Cyclic voltammetry was carried out using an EG & G model 362 potentiostat and the Condecon 310 software package, with *ca.* 10^{-3} mol dm^{-3} solutions under dry N_2 in dry dichloromethane or acetonitrile. A Pt bead working electrode was used, with 0.2 mol dm^{-3} [*n*-Bu_4N][BF_4] as supporting electrolyte, and a scan rate of 200 mV s^{-1}. Potentials were recorded *vs.* a saturated calomel reference electrode, and ferrocene ($E_f = 0.55 \pm 0.01$ V in dichloromethane) was added as an internal standard. The data obtained were reproducible, the experimental error being ± 10 mV.

All spectroelectrochemical studies were carried out using an Autolab System containing a PSTAT20 potentiostat, using General Purpose Electrochemical System (GPES) Version 4.5 software. Positive feedback ohmic compensation was applied for all cyclic voltammograms recorded. All solutions were purged with Ar for 20 minutes prior to study. Electrogeneration potentials of the reduction processes were at more negative values than the E_f of the couple.

The optically transparent electrode cell (O.T.E.) for use in UV/vis/near-IR spectrometers has been described previously.[9] EPR spectra were recorded on an X-band Bruker ER200DSCR spectrometer, using the *in-situ* cell described previously.[10] EPR simulations are performed using WINEPR SimFonia.[11]

Microanalyses were performed by the University of North London.

Syntheses

5,10,15,20-(4-Pyridyl)triphenylporphyrin, 1. Pyridine-4-carbaldehyde (8.0 ml, 68.0 mmol) and benzaldehyde (6.0 ml, 57.6 mmol) were added to propionic acid (450 ml) in a 2 l three-neck round-bottom flask. The flask was equipped with two condensers and an overhead stirrer. The mixture was stirred and brought to reflux. Freshly-distilled pyrrole (8.8 ml, 127.0 mmol) was added dropwise over a period of 45 minutes and then the resulting mixture was stirred under reflux for 1 hour. The mixture was then left to cool for 18 hours. The purple mixture of products was separated from the black solution by vacuum filtration.

The products were separated using column chromatography. The first band (tetraphenylporphyrin) was eluted using dichloromethane (3 l). The desired product was collected as the second band, eluting with 1% methanol in dichloromethane (5 l). The solvent was removed *in vacuo* to give a purple solid. Yield: 0.83 g (4.25%). ^{1}H NMR (300 MHz, $CDCl_3$ *cf.* Chart 1 for ring and atom labelling): δ 9.04 (2H, d, $^{3}J = 5.1$ Hz, pyridine H_a and $H_{a'}$), 8.86 (4H, A_2B_2, $J_{AB} = 4.8$ Hz, $\Delta\delta_{AB} = 0.10$ ppm, pyrrole protons of rings A and B), 8.88 (4H, s, pyrrole protons of rings C and D), 8.22–8.24 (6H, m,

ortho protons of Ph in Ph_3-porphH_2), 8.19 (2H, d, $^3J = 5.5$ Hz, pyridine H_b and $H_{b'}$), 7.76–7.78 (9H, m, *meta* and *para* protons of Ph in Ph_3-porphH_2), −2.79 (2H, s, central N*H* of porphyrin ring). Found: C, 84.0; H, 4.9; N, 11.3. Calc. for $C_{43}H_{29}N_5$: C, 83.9; H, 4.8; N, 11.4%. LSIMS: *m/z* 616 ([M]$^+$).

***N*-Benzyl-4-pyridinium-4′-pyridine hexafluorophosphate, 2.** 4,4′-Bipyridyl (3.75 g, 24 mmol, 2.0 equiv.) was dissolved in warm toluene (100 ml) and heated with stirring to 80 °C. Benzyl bromide (2.00 g, 12 mmol, 1.0 equiv.) was dissolved in toluene (20 ml) and added to the mixture over a period of 3 hours. The reaction was then refluxed with stirring for 18 hours. The resulting yellow precipitate was filtered hot under vacuum and left to air-dry. The residue was dissolved in warm deionised water (40 ml) and a saturated solution of NH_4PF_6 was added until no further precipitation was observed. The off-white precipitate was filtered off under vacuum, washed with deionised water and dried in a vacuum desiccator to give the pure product. Yield: 2.15 g (45.4%). ^{1}H NMR (300 MHz, d_6-acetone *cf.* Chart 1 for ring and atom labelling): δ 9.35 (2H, d, $^3J = 7.0$ Hz, H_α and $H_{\alpha'}$), 8.86 (2H, d, $^3J = 5.2$ Hz, H_ε and $H_{\varepsilon'}$), 8.68 (2H, d, $^3J = 6.6$ Hz, H_β and $H_{\beta'}$), 7.99 (2H, d, $^3J = 5.9$ Hz, H_χ and $H_{\chi'}$), 7.65–7.68 (2H, m, phenyl ring *ortho* positions), 7.49–7.52 (3H, m, phenyl ring *meta* and *para* positions), 6.11 (2H, s, CH_2). Found: C, 52.3; H, 3.7; N, 7.0. Calc. for $C_{17}H_{15}N_2PF_6$: C, 52.1; H, 3.9; N, 7.1%. LSIMS: *m/z* 247 ([M − PF_6]$^+$).

5,10,15,20-[N-(4-Bromomethylbenzyl)-4-pyridyl]triphenylporphyrin hexafluorophosphate 3. Compound **1**, (0.33 g, 5.33×10^{-4} mol, 1.0 equiv.) and α,α′-dibromo-*p*-xylene (1.67 g, 6.67×10^{-3} mol, 12.5 equiv.) were dissolved in dry THF (70 ml) and heated to reflux under nitrogen for 6 hours. The reaction mixture was then left to cool with stirring for 18 hours. The resulting solution was evaporated to half of its original volume *in vacuo* and then a saturated solution of NH_4PF_6 was added until no further precipitation was seen. The mixture was filtered under vacuum and allowed to air-dry. The crude product was separated from the residual starting materials by column chromatography, eluting with 1% methanol in dichloromethane (2.5 l). The solvent was removed to afford **3** as a purple solid. Yield: 0.14 g (28.2%). ^{1}H NMR (300 MHz, CD_3CN *cf.* Chart 1 for ring and atom labelling): δ 9.07 (2H, d, $^3J = 6.6$ Hz, pyridine H_a and $H_{a'}$), 8.92 (4H, A_2B_2, $J_{AB} = 4.8$ Hz, $\Delta\delta_{AB} = 0.10$ ppm, pyrrole protons of rings A and B), 8.82–8.85 (4H, m, pyrrole protons of rings C and D), 8.77 (2H, d, $^3J = 6.6$ Hz, pyridine H_b and $H_{b'}$), 8.17–8.21 (6H, m, *ortho* protons of Ph in Ph_3-porphH_2), 7.98 (4H, A_2B_2, $J_{AB} = 7.4$ Hz, $\Delta\delta_{AB} = 0.22$ ppm, phenyl ring E), 7.78–7.82 (9H, m, *meta* and *para* protons of Ph in Ph_3-porphH_2), 6.00 (2H, s, H_c and $H_{c'}$), 4.70 (2H, s, H_d and $H_{d'}$), −2.86 (2H, s, central N*H* of porphyrin ring). Found: C, 64.8; H, 4.1; N, 7.6. Calc. for $C_{51}H_{37}N_5BrPF_6$: C, 64.8; H, 4.0; N, 7.4%. LSIMS: *m/z* 800 ([M − PF_6]$^+$), 616 ([M − C_8H_8Br − PF_6]$^+$).

5,10,15,20-[*N*-benzyl-*N*′-(4-benzyl-4,4′-bipyridinium-4-pyridyl)]triphenylporphyrin tris(hexafluorophosphate), 4. Compound **3** (0.10 g, 1.06×10^{-4} mol, 1.0 equiv.) and compound **2** (0.64 g, 1.63×10^{-3} mol, 14.0 equiv.) were dissolved in dry acetonitrile (50 ml). The mixture was stirred under reflux for 12 hours under an atmosphere of nitrogen and then left to cool. The volume of the resulting solution was reduced to half under vacuum, then a saturated solution of NH_4PF_6 was added until no further precipitation was seen. The crude product was collected by vacuum filtration and purified by column chromatography (methanol, $NH_4Cl_{(aq)}$ [2.0 M], nitromethane; ratio of 7 : 2 : 1). The desired product was collected as the major coloured band. Solvent was removed under vacuum and residual solid NH_4Cl was removed by washing with water. The product was dissolved in dichloromethane and dried over $MgSO_4$. The pure product was obtained as a red-purple solid. Yield: 0.11 g (71.3%). ^{1}H NMR (400 MHz, d_6-acetone, see Chart 1 for ring and atom labelling): δ 9.64 (2H, d, $^3J = 6.5$ Hz, H_a and $H_{a'}$ of porphyrin pyridine ring), 9.52 (2H, unresolved, H_ε and $H_{\varepsilon'}$ of 4,4′-bipyridine), 9.49 (2H, d, $^3J = 5.3$ Hz, H_α and $H_{\alpha'}$ of 4,4′-bipyridine) 9.12 (2H, d, $^3J = 6.6$ Hz, H_b and $H_{b'}$ of porphyrin pyridine ring), 9.00 (2H, d, $^3J = 4.7$ Hz, H_χ and $H_{\chi'}$ of 4,4′-bipyridine), 8.94 (2H, d, $^3J = 4.7$ Hz, H_β and $H_{\beta'}$ of 4,4′-bipyridine), 8.87–8.91 (4H, m, pyrrole protons of rings A and B), 8.81–8.83 (4H, m, pyrrole protons of rings C and D), 8.22–8.26 (6H, m, *ortho* protons of Ph in Ph_3-porphH_2), 8.00 (4H, A_2B_2, $J_{AB} = 8.2$ Hz, $\Delta\delta_{AB} = 0.12$ ppm, phenyl ring E), 7.81–7.88 (9H, m, *meta* and *para* protons of Ph in Ph_3-porphH_2), 7.64–7.67 (2H, m, *ortho* protons of phenyl ring F), 7.48–7.50 (3H, m, *meta* and *para* protons of phenyl ring F), 6.45 (2H, s, H_c and $H_{c'}$), 6.30 (2H, s, H_d and $H_{d'}$), 6.17 (2H, s, H_e and $H_{e'}$), −2.74 (2H, s, central N*H* of porphyrin ring). ^{13}C NMR (125 MHz, CD_3CO): δ 65.3 (*C*[H_c]$_2$), 65.8 (*C*[H_d]$_2$), 66.5 (*C*[H_e]$_2$), {113.5, 123.1, 124.2}, 128.6 and 128.7 (*meta* and *para* *C*H of Ph in Ph_3-porphH_2), 129.2 and 129.3 (*C*H of pyrrole rings C and D), 129.9 (*meta* and *para* *C*H of Ph in Ph_3-porphH_2), 131.0 (*C*H of phenyl ring F), 131.3 (*C*H_b of porphyrin pyridine ring), 131.8 (*C*H of phenyl ring F), 132.1 and 132.5 (*C*H of phenyl ring E), {133.4, 134.2}, 134.4 and 135.1 (*C*H of pyrrole rings A and B), 136.0 (*ortho* *C*H of Ph in Ph_3-porphH_2), {136.3, 142.9, 143.0}, 144.5, 147.2 and 147.4 (*C*H_a of porphyrin pyridine ring and *C*$H_{\alpha,\varepsilon}$), {152.0, 152.3, 161.7}. Found: C, 58.4; H, 3.9; N, 6.9. Calc. for $C_{68}H_{52}N_7P_3F_{18}$: C, 58.3; H, 3.7; N, 7.0%. LSIMS: *m/z* 1402 ([M]$^+$), 1256 ([M − PF_6]$^+$), 1111 ([M − 2PF_6]$^+$).

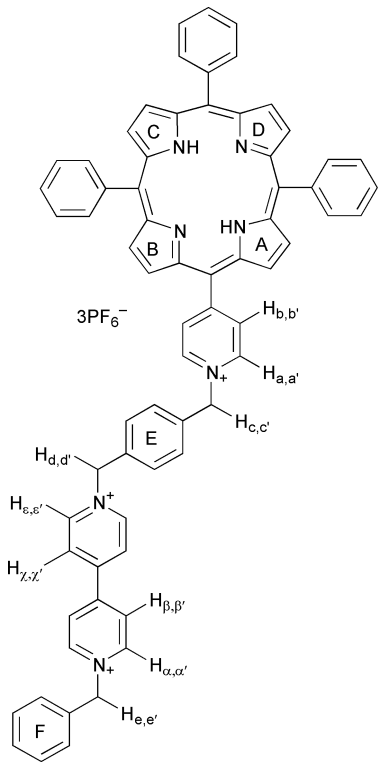

Chart 1 Atom labelling in diad **4**.

Conclusions

In summary, we have described the design, synthesis and characterisation of a new potentially photoactive donor–acceptor diad compound **4** and its precursors. *In-situ* UV/Visible and EPR measurements have shown that the site of the first electrochemical reduction is the benzylviologen component of the molecule. The second reduction wave from cyclic voltammetry

was shown by *in-situ* EPR to comprise two unresolved one-electron processes. The first of the two electron reduction processes rendered the diad diamagnetic, as was shown by the disappearance of the signal due to the benzylviologen radical. The second of these processes gave rise to the appearance of a new EPR signal, which was found to correspond to the porphyrin radical. We believe this to be the first reported resolved spectrum of a monoreduced porphyrin radical. This is a significant step towards our ultimate aim of assembling zeolite-occluded diads in order to attempt the photogeneration of long-lived charge separated states.

Acknowledgements

We thank the EPSRC (UK) for financial support.

References

1 N. M. Rowley, S. S. Kurek, M. W. George, P. D. Beer, S. M. Hubig, C. J. Jones, J. M. Kelly and J. A. McCleverty, *J. Chem. Soc., Chem. Commun.*, 1992, 497.
2 N. M. Rowley, S. S. Kurek, J.-D. Foulon, T. A. Hamor, C. J. Jones, J. A. McCleverty, S. M. Hubig, E. J. L. McInnes, N. N. Payne and L. J. Yellowlees, *Inorg. Chem.*, 1995, **34**, 4414.
3 N. M. Rowley, S. S. Kurek, P. R. Ashton, T. A. Hamor, C. J. Jones, N. Spencer, J. A. McCleverty, G. S. Beddard, T. M. Feehan, N. T. H. White, E. J. L. McInnes, N. N. Payne and L. J. Yellowlees, *Inorg. Chem.*, 1996, **35**, 5526.
4 (*a*) R. J. McMahon, R. K. Forcé, H. H. Patterson and M. S. Wrighton, *J. Am. Chem. Soc.*, 1988, **110**, 2670; (*b*) R. K. Forcé, R. J. McMahon, J. Yu and M. S. Wrighton, *Spectrochim. Acta., Sect. A*, 1989, **45**, 23.
5 E. H. Yonemoto, Y. I. Kim, R. H. Schmehl, J. O. Wallin, B. A. Shoulders, B. R. Richardson, J. F. Haw and T. E. Mallouk, *J. Am. Chem. Soc.*, 1994, **116**, 10557.
6 A. D. Adler, F. R. Longo, J. D. Finarelli, J. Goldmacher, J. Assour and L. Korsakoff, *J. Org. Chem.*, 1967, **32**, 476.
7 R. H. Felton and H. Linschitz, *J. Am. Chem. Soc.*, 1966, **88**, 1113.
8 M. Low, PhD thesis, University of Edinburgh, 1987.
9 D. Collison, F. E. Mabbs, E. J. L. McInnes, K. J. Taylor, A. J. Welch and L. J. Yellowlees, *J. Chem. Soc., Dalton Trans.*, 1996, 329.
10 E. J. L. McInnes, R. D. Farley, C. C. Rowlands, A. J. Welch, L. Rovatti and L. J. Yellowlees, *J. Chem. Soc., Dalton Trans.*, 1999, 4203.
11 WINEPR SimFonia, version 1.25, Bruker Analytische Messtechnik GmbH, 1996.